COMPARATIVE STUDY OF ACOUSTIC EMISSION SIGNALS FROM WOOD SPECIMENS UNDER STATIC BENDING LOAD

David VARNER[*], Miroslav VARNER [**]

[*] Department of Engineering and Automobile Transport, Faculty of Agronomy, Mendel University, Brno, Czech Republic, [**] CorrosionFatigue Association

Contact e-mail: info@davar.cz

Abstrakt

V článku jsou prezentovány výsledky měření signálů akustické emise během standardní ohybové zkoušky dřevěných vzorků. Pro pět typů dřeva byly identifikovány typické průběhy vzniku akustické emise. Na základě těchto poznatků bude v průběhu dalšího výzkumu proveden odhad chování jednotlivých vzorků a vznik porušení při ohybovém zatížení. Ortotropní vlastnosti dřeva ovlivňují významnou měrou možnost použití známých technik monitorování a vyhodnocení signálů AE. Při měření byly u vzorků zjišťovány další vlastnosti, zejména modul pružnosti, mez pevnosti, délka namáhání a hustota. Výsledky budou prezentovány v rámci disertační práce zaměřené na nedestruktivní diagnostiku porušení dřeva metodou akustické emise.

Klíčová slova: dřevo, zkouška statickým ohybem, akustická emise

Abstract

In this innovative study, acoustic emission signals were captured during commonly used static bending test of wood specimens. For five different wood types, typical AE patterns were identified in the acoustic emission records to further describe the under-the-stress behavior and failure development. Orthotropic properties of wood were found to be rather complicated to conform within known AE techniques. Evaluated properties of the material included MOE (modulus of elasticity), MOR (modulus of rapture), TTF (time to failure), and density. Results of the study will be included in a dissertation thesis focused on non-destructive diagnostics of wood using acoustic emission method.

Keywords: wood, static bending test, acoustic emission

Introduction

Acoustic emissions are the stress waves produced by the sudden internal stress redistribution of the materials caused by the changes in the internal structure. Possible causes of the internal-structure changes are crack initiation and growth, crack opening and closure, dislocation movement, twinning, and phase transformation in monolithic materials and fiber breakage and fiber-matrix debonding in composites. Most of the sources of AEs are damage-related; thus, the detection and monitoring of these emissions are commonly used to predict material failure. [2]

In technical diagnostics, AE method has been used to monitor rotational part status (friction and cavitation of bearings/gears), detection of micro-cracks, pressure vessel defects, tubing system defects, aircraft structure evaluation/testing, and bridge status diagnostics. AE technique has proven useful in fatigue testing and destruction experiments.

Major advantages of AE include continuous monitoring of the object, time savings, and failure forecast abilities. On the other hand, AE wave source is not always obvious, as the emitted energy may result from several phenomena inside of the part. Further variable factors include shape of the object, surface area, material structure, and homogeneity level. [2]

Two important issues in AE monitoring technique during bending tests are source identification and damage quantification. A standard bending test samples were used in the experiments. For damage quantification, two methods were used to analyze experimental data: b-value analysis and intensity analysis. [1]

Loading conditions during the static bending might be crucial for the stress distribution and response of the specimen. MOE (modulus of elasticity) and MOR (modulus of rupture) may differ based on the loading configuration. Two types of loading were established: LR beams (annual rings horizontal, load applied to LT face) and LT beams (annual rings vertical, load applied to LR face). The size of the specimens was 10 x 10 x 150 mm. It was found that the variation of MOE and MOR was lower with loads applied to the longitudinal-radial face than the longitudinal-tangential face. Additional information was received about the influence of earlywood and latewood on the tension/compression surfaces. [3]

Methodology based on count and properties of annual rings was used in series of experiments including static bending test of cypress wood samples. Relationship between number of annual rings in the specimen cross-section, wood density, and strength properties of the wood specimens was calculated together with modulus o elasticity (MOE) and modulus of rupture (MOR). [4]

It is apparent that the span/depth ratio for bending test specimens can influence the test as well. This behavior was examined with specimens made from Japanese fir. Several material properties were evaluated during modified three-point and four-point bending tests. These included Young's modulus, proportional limit stress, and bending strength Deflection was measured using three different methods Authors found that the span/depth ratio should be larger than 20 to produce bending properties conforming well to the elementary bending theory. The changes of the ratio seemed to have significant influence on measurements of Young's modulus. [5]

Experimental Setup

According to the standard [7], static bending test procedure is performed to find ultimate static bend load causing permanent damage of the tested specimen. Testing specimens must be in form of regular-shaped boxes with base dimensions of 20 x 20 mm and length of 300 mm. The fiber direction has to correspond with length dimension. The bending strength is calculated in N/m^2 or kp/cm^2. Calculated values are usually adjusted to 12% moisture content.

For the actual static bending test, 50 specimens were used. The wood types used were 3 hardwoods (beech, oak, poplar) and 2 softwoods (spruce, pine). For each wood type, 10 specimens were prepared. The specimens were carefully selected with maximum possible uniformity requirements in mind. However, not every specimen had exactly the same structure as the others. Sometimes the annual rings were slightly angled; some specimens had different surface roughness etc.

As far as the specimen moisture content is concerned, the specimens had been stored in a storage facility with stabile ambient conditions.

In static bending test procedure, the specimen was placed on two supports at the ends while the third point provided downward pressure in the midpoint. The forces from above acted in radial direction, i.e. the rings were close to horizontal. This test is called three-point bending test in some publications. It has been used for testing of wide range of materials including steel and plastics. There are some variations of the test, e.g. the rings can be vertical in the loading position.

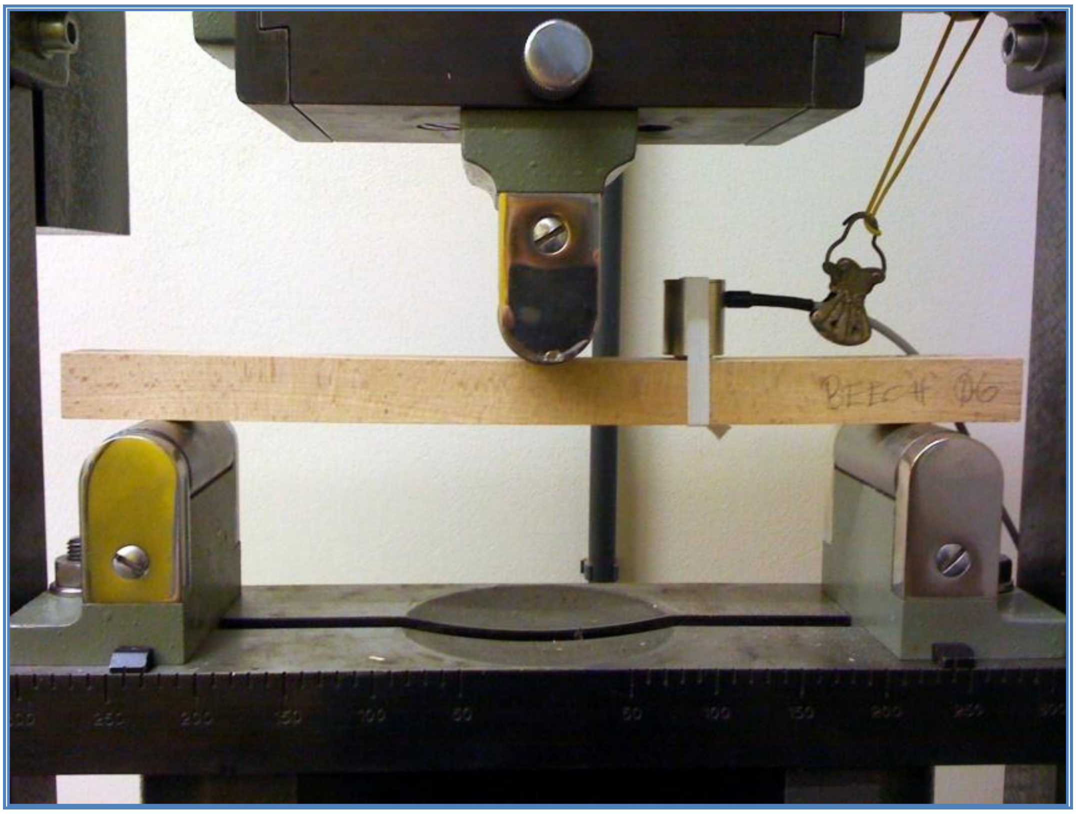

Figure 1: Position of a wood specimen on the bending test machine. Note the AE 767 acoustic emission sensor attached to the specimen via a rubber band and secured against fall-down using a security clamp.

Prior to actual testing, several issues had to be addressed including synchronous recording of the bending test machine and AE signal. Sensor safety precautions were taking into account as well. Preliminary trial test runs revealed possibility of total destruction of the specimen (probably due to internal imperfections or defects). In such case, the remains of the specimen could fall down from the bending machine resulting in severe sensor damage. A simple sensor holder was used to prevent this scenario: a clamp was attached to the sensor cable and fixed using a rubber band. In case of specimen destruction, the sensor was supposed to remain hanging on the machine frame. The actual static bending test procedure was as follows:

- Specimen was selected from the storage facility and designated by wood type and number. Specimen dimensions and weight were measured.
- A slight film of silicone grease was applied to the contact surface and a single sensor was fixed to the specimen using a rubber band, with the distance from the midpoint being 10 cm.
- The specimen was placed onto the bending test machine. The appropriate position was adjusted visually.
- The test run was performed until final breakage of the specimen. After starting the test, the AE monitoring was simultaneously triggered. The bending test progress was viewed on-screen of the PC. During the test, several photos were

taken to follow the change of shape and fracture development. Average test run time was 90 seconds.

- Then, specimen was removed from the bending test machine and photographed. Pressure traces on the specimen contact surfaces were measured.
- Data from the bending test were logged and merged into the Dakel Daeshow software. AE RMS vs. time plots were created for individual testing runs.
- Supplementary properties of the testing specimens were calculated including MOE (modulus of elasticity), MOR (modulus of rupture), and density.

Instrumentation and Equipment

The acoustic emission was monitored using Dakel XEDO AE analyzer, a single Dakel sensor and Dakel Daemon software. A 35 dB pre-amplifier was connected to a special low frequency slot in the Dakel XEDO analyzer. The slot was adjusted to cover the frequency range of 10 - 200 kHz. A cylinder-shaped Dakel AE 469 sensor was used for all the bending test runs.

For the static bending test, the ZDM 5/51 machine was used. This machine uses electric power unit and spiral gear drive to lift the bridge with lower support assembly. The device has been installed in the Department of Wood Science laboratory. The ZDM 5/51 bending test machine was equipped with a PC terminal with the M-Test 1.77 software for test control purposes.

Static Bending of Wood

Behavior of the specimen during the static bending test is quite variable with respect to orthotropic nature of the material. The longitudinal axis L is parallel to the wood fiber (grain); the radial axis R is normal to the growth rings (perpendicular to the grain in the radial direction); and the tangential axis T is perpendicular to the grain but tangent to the growth rings. Each of the directions holds unique property set.

During the static bending test, the wood specimen is exposed to compression stress on one surface and tensile stress on the other. This complicated distribution of stress results in a various shear displacements within the cross-section of the beam. Due to anisotropic structure, acoustic emission generated during clear wood damage process shows parameters dependent on loading type and its orientation with respect to grain direction.

When tensile load is being applied in the grain direction, the acoustic emission is expected to come from several sources including separation of cellulose micro fibrils and lignin matrix, actual micro fibril breakage, and final fracture of the entire cell wall.

In perpendicular direction, the cell walls are less reinforced with micro fibrils and overall cell wall strength is reduced. When a tensile loading is applied in this direction, it is likely that acoustic emission signals originate in degradation-related changes of cell wall lignin mass.

Final stage fracture always generates peak acoustic emission bursts (even in audible spectra range). This moment corresponds to MOR (modulus of rupture) ultimate loading conditions.

The procedure listed above applies to wood in general. Obviously, there are different bending failure mechanisms for hardwood and softwood as defined by different wood structure. Microstructure of a hardwood specimen contains vessels, fibers and parenchyma cells, while the tracheids are very few in numbers. In softwood however, there are just two cell types sharing support, conduction and storage functionality: parenchyma cells and tracheids.

Sources of Acoustic Emission during the Static Bending Test

In general, acoustic emission may come from several sources in context of the static bending test: bending machine noise, contact-surface friction noise, gradual collapsing of wood cell walls, and final fracture of the specimen body.

The first two noise types in the list are obviously undesirable. To reduce their influence, it was decided to carry-out a low-friction modification of the static bending test using a low-friction material (10 mm wide Teflon tape) on the contact surfaces. The presumption was that the Teflon tape would not only act as a friction reduction element, but as an "acoustic barrier" as well. After the testing, acoustic emission RMS vs. loading force plots were compared for regular specimens and T (Teflon-tape) specimens.

Results

As expected, the experiment showed quite a different behavior of individual wood type specimens subject to static bending test. In this very first phase of the research, acoustic emission RMS vs. loading force plots were created for each of the 50 regular specimens and 5 Teflon-tape specimens. The aim was to overview the plots and find typical patterns for future observations.
Property parameters of the specimens and static bending test itself included actual moisture content, density, TTF (time to failure), Fmax (maximum loading force at ultimate strength level), MOE (modulus of elasticity in bending) and MOR (modulus of rupture in bending). As far as the low friction modification of the static bending test is concerned, no significant influence was indicated from the plots. Below you can find table with overview of average property values.

Wood Type	**MC (%)**	**Density (kg/m3)**	**TTF (sec)**	**Fmax (N)**	**MOE (MPa)**	**MOR (MPa)**
Oak	7,6	662,5	59,4	2178,5	11076,5	106,8
Beech	6,2	670,9	73,1	2998,3	11866,7	129,4
Poplar	7,6	383,8	74,7	1394,7	6880,0	66,7
Pine	6,8	499,0	100,4	2085,3	10662,1	94,3
Spruce	8,7	525,0	73,3	1875,7	9233,0	84,7

Table 1: Average property values for individual wood type groups.

OAK Specimens can be divided into 2 behavior-specific groups. 3 specimens showed no AE activity was recorded during the entire bending run; they remained silent until the major fracture. The rest of the testing group showed strong pulses in 80% of ultimate load. The OAKT specimen bore the highest loading force value of 3151 N with very silent pre-fracture phase until 90% of ultimate load. OAK wood breakage resembled to simple-tension type failure with short horizontal portions parallel to grain and vertical bridging perpendicular to grain. On some specimens, kinking bands were visible under upper loading support. Typical OAK specimen plot can be seen in figure below.

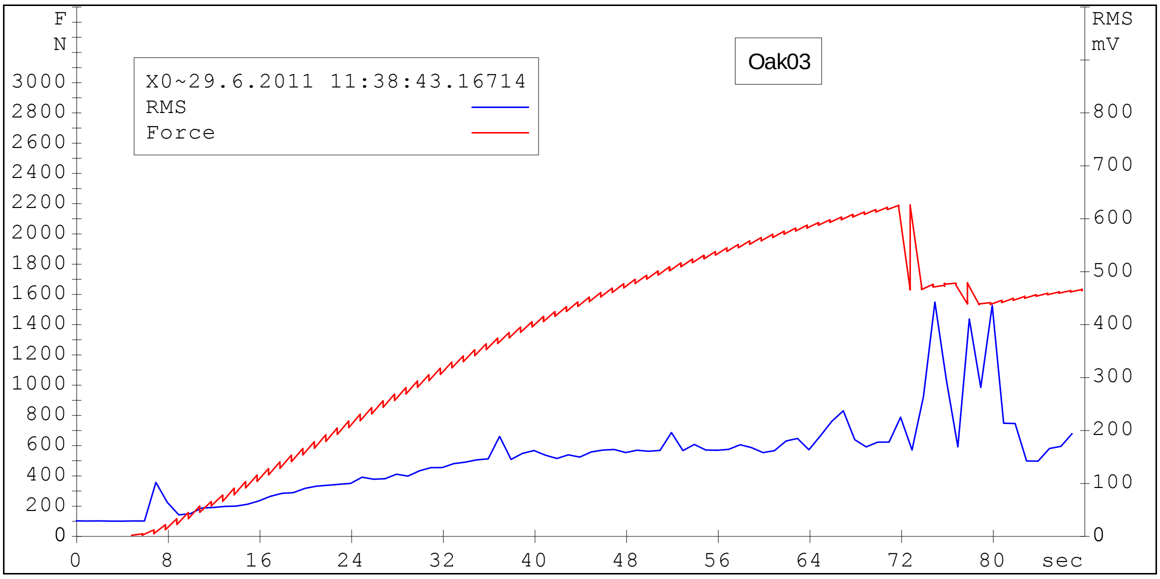

Figure 2: Typical plot of loading force vs. AE RMS for OAK specimen group.

BEECH Specimens showed Live AE activity during transition from elastic to plastic phase and very high values of loading force. BEECH09 specimen withstood the highest loading force of the entire testing set of 50 specimens, reaching value over 3700 N. The BEECHT specimen showed significant differences, reaching loading force value of 3070 N. Fracture type was simple tension (6 specimens) and cross-grain failure (4 specimens). Typical BEECH specimen plot can be seen in figure below.

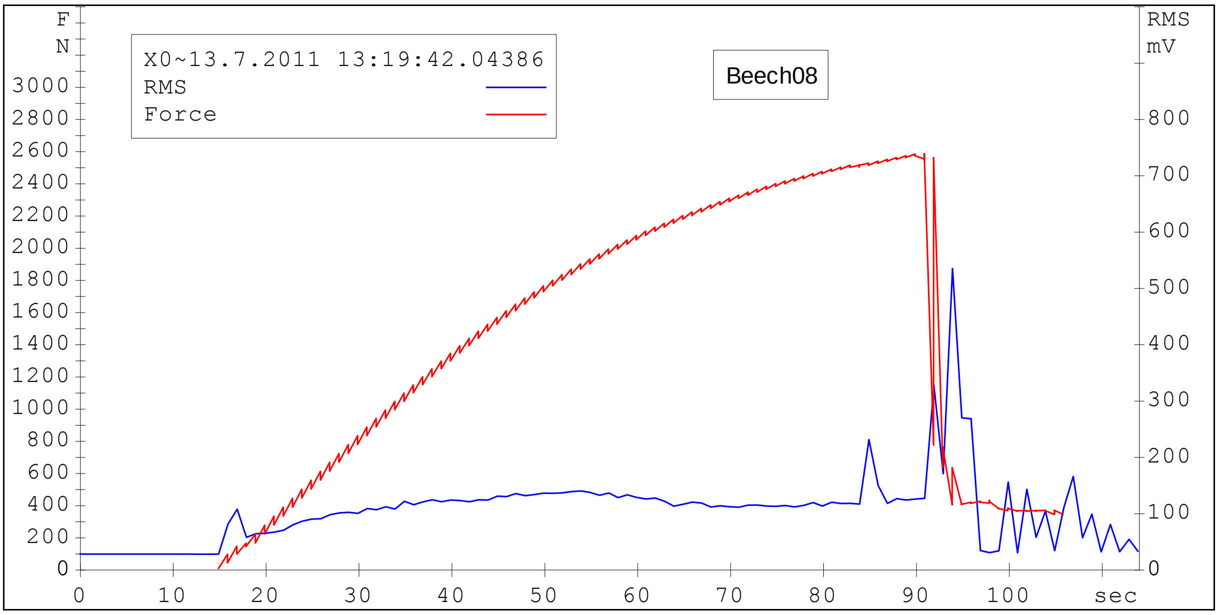

Figure 3: Typical plot of loading force vs. AE RMS for BEECH specimen group.

POPLAR was the final hardwood type to be subject to the static bending test. As indicated by table 1 data, the specimens reached the lowest MOE/MOR values from all the wood types. Fracture types included splintering tension (6 specimens), simple tension (3 specimens), and massive cross-grain failure (1 specimen). Loading force vs. AE RMS plots of POPLAR specimens show high level of uniformity with only one exception: POPLAR01 specimen showed short extreme AE activity around 25% of ultimate load. The reason for this unstable behavior is not known, most probably there was some external unwanted source of AE signals. The POPLART specimen was perfectly uniform with the rest of the group. Typical POPLAR specimen plot can be seen in figure below.

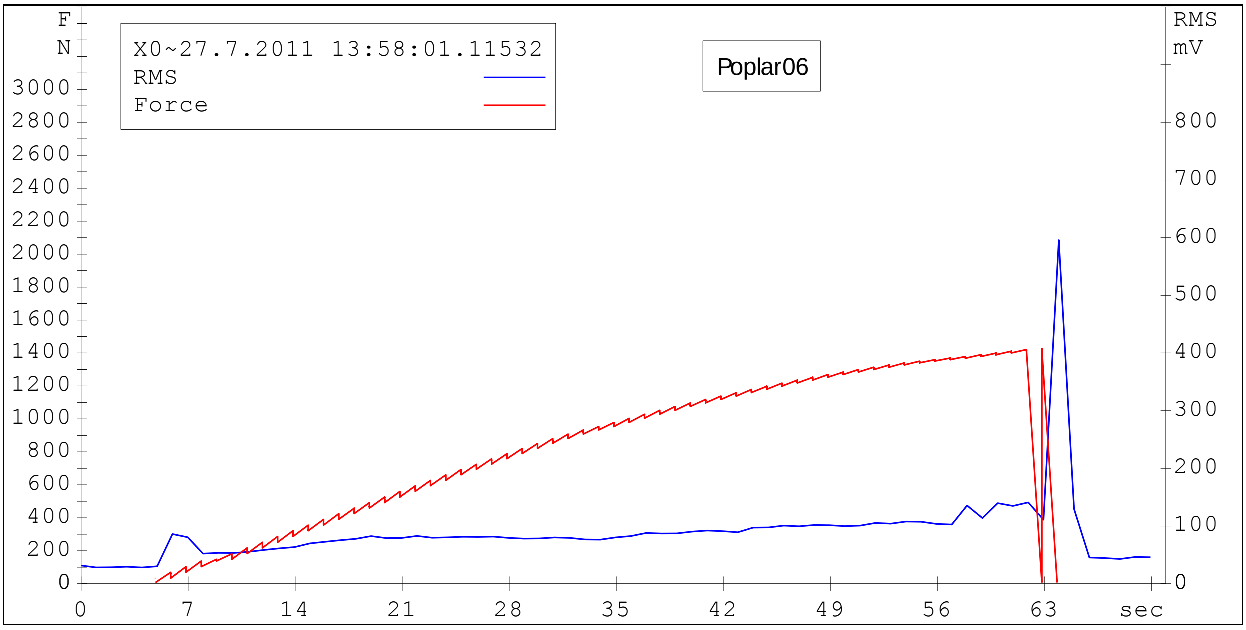

Figure 4: Typical plot of loading force vs. AE RMS for POPLAR specimen group.

PINE specimens showed very distinctive behavior under severe static bending load. 7 out of 10 specimens registered strong AE activity starting from 20% of ultimate load. The Teflon-equipped PINET specimen was described by a flat AE response with 5 isolated peaks of AE activity. As far as the fracture of specimens is concerned, the PINE group showed strong affinity to parallel-to-grain delamination along annual rings (7 specimens out of 10). The rest of the specimen failed in non-specific manner. It is worth noting that PINE group specimens were found the most “compressible” with ratio of 1/10. Typical PINE specimen plot can be seen in figure below.

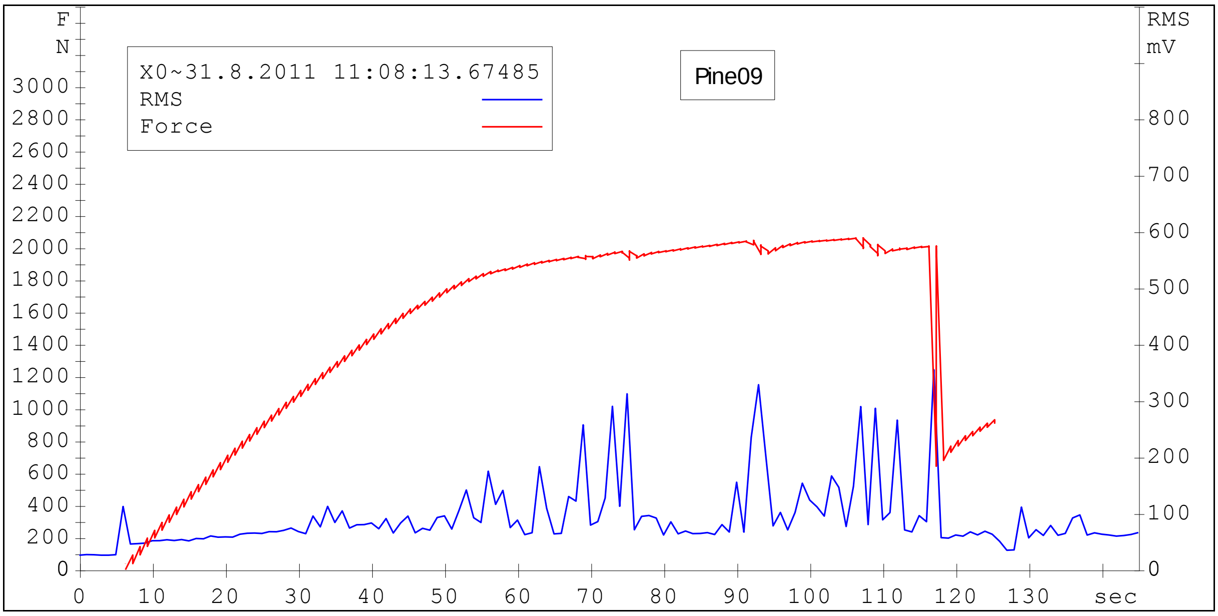

Figure 5: Typical plot of loading force vs. AE RMS for PINE specimen group.

SPRUCE specimen group represented the most diversified set of under-the-load behavior. 3 specimens showed interesting trend of multiple minor failures and hardening prior to final master failure. The minor failures marked the ultimate strength of the specimen. However, there was a strong residual rigidity in comparison with other wood type groups. As far as the fracture type of PINE group is concerned, it was rather difficult to find a pattern there as well. Most of the specimens failed in a combination of plain tension and massive cross-grain destruction.

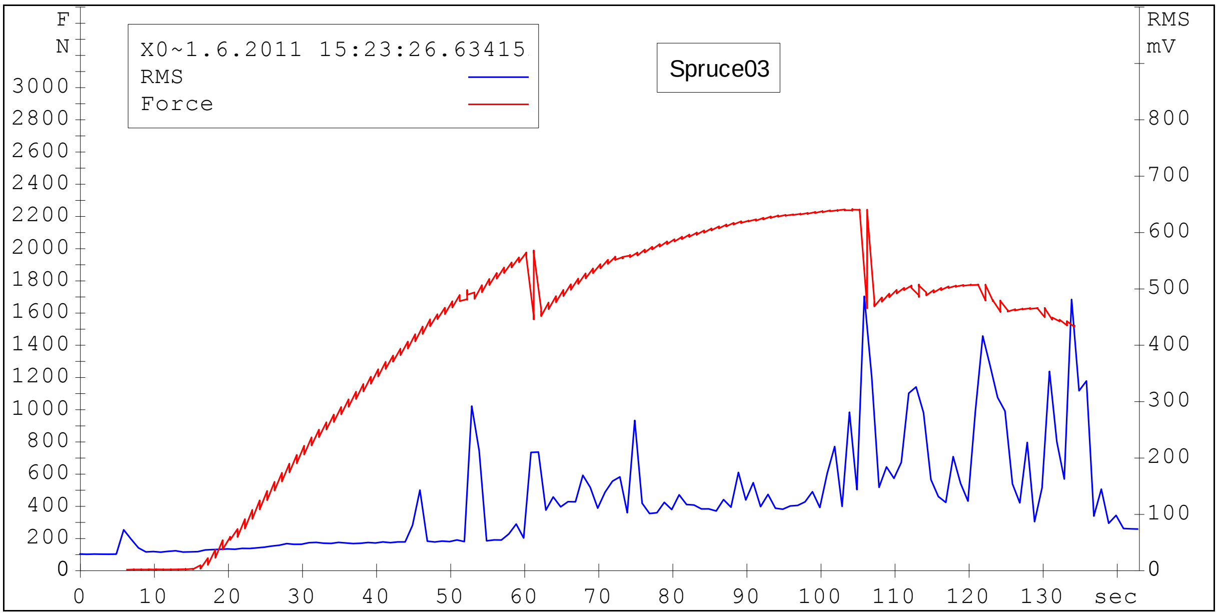

Figure 6: Typical plot of loading force vs. AE RMS for SPRUCE specimen group.

Conclusions

Acoustic emission method has been used to describe under-stress behavior of 5 wood type specimens during a static bending test. Essential methodology guidelines were elaborated with respect to complicated material properties and structure of wood. However, not all issues were successfully resolved.

As there is no way of performing a perfectly “standard” bending test, some compromises are needed to establish general rules for the procedure. On the other hand, this experiment simulates “real-life” conditions and materials that can be found in the wood processing industry.

Next phase of research will include analysis of frequency variations for individual AE events recorded from different wood types. Results of this study will form an integral part of dissertation thesis dedicated to assessment of wood properties using acoustic emission method.

References

[1] KAPHLE, S. R.; TAN, A. C. C.; Thambiratnam, D. P; Chan, T. H.T.: Study of Acoustic Emission Data Analysis Tools for Structural Health Monitoring Applications. In: Progress in Acoustic Emission XV : Proceedings of the 20th International Acoustic Emission Symposium [online]. Kumamoto, Japan. 2010

[2] KREIDL, Marcel, ŠMÍD, Radislav. Technická diagnostika. 1. vyd. Praha : Nakladatelství BEN, 2006

[3] GROTTA, T. A.; LEICHTI, R. J.; GARTNER, B. L.; JOHNSON, G. R.: Effect of growth ring orientation and placement of earlywood and latewood on MOE and MOR of very-small clear Douglas-fir beams. Wood and Fiber Science, 37(2). 2005

[4] KIAEI, M.; VEYLAKI, M.: Relationship Between Number of of Annual Rings In Sample Cross-Section And Static Bending Strength of Cypress Wood by Linear and Power Models. World Applied Sciences Journal 13 (2). 2011.

[5] YASHIHARA, H.; KUBOJIMA, Y.; ISHIMOTO, T.: Several examinations on the static bending test methods of wood using todomatsu (Japanese fir). Forest Products Journal. 2003

[6] POŽGAJ, A.: Štruktúra a vlastnosti dreva. 1.vyd. /. Bratislava : Príroda, 1993. 485 pages. ISBN 80-070-0600-1.

[7] ČSN 49 0115. Wood. Determination of ultimate strength in flexure tests. Praha : Vydavatelství Úřadu pro normalizaci a měření, 1979. 6 pages.

Acknowledgements

Authors would like to thank the Dakel ZD Rpety Company for AE equipment support.